https://doi.org/10.15446/recolma.v56n2.108369

Revista Colombiana de Matemáticas
Volumen 56(2022)2, páginas 113-131

Population dynamics with protection and harvesting of a species

Dinámica poblacional con protección y explotación de una especie

Christian Camilo Cortes[1, 2,✉], Juan David Hernandez[3]

[1]Universidad Carlos III de Madrid, Madrid, España

[2]Centro Nacional de Biotecnología, Madrid, España

[3]Universidad Surcolombiana, Neiva, Colombia

Abstract. In this work we study the dynamics associated to the interaction of juveniles and adults of the same species, where the harvesting of adults is not allowed when the number of adults is below a critical value. This study is carried out by bifurcation analysis, for a Filippov system, in relation to two parameters: harvesting and protection of the adult species.

Key words and phrases. Filipov systems, bifurcation, sliding segment, Poincare-Bendixson criteria, limit cycle.

2020 Mathematics Subject Classification. 34A36, 34C23, 34D20, 34D23, 92D25.

Resumen. En este trabajo se estudia la dinámica entre la interacción de jóvenes y adultos de una misma especie, donde la explotación de los adultos no es permitida cuando el número de adultos es inferior a un valor crítico. Este estudio es llevado a cabo por el análisis de bifurcación, para un sistema de Filippov, con relación a dos parámetros: explotación y protección de la especie adulta.

Palabras y frases clave. Sistemas de Filippov, Bifurcación, segmento deslizante, criterio de Poincare-Bendinxson, ciclo limite.

1. Introduction

A great variety of phenomena in nature are modeled using systems of differential equations of the form

$$\dot{u} = f(u)$$

where $f : \mathbb{R}^n \to \mathbb{R}^n$ is a continuous and differentiable vector field. In particular, these systems are used to explain the dynamics between species that inhabit the same environment to determine whether or not they become extinct over time [2, 8].

However, many ecological phenomena are modeled by discontinuous dynamical systems, called *Filippov systems* [3], described by autonomous differential equations of the form:

$$\dot{u} = \begin{cases} f_1(u), & u \in S_1 \subset \mathbb{R}^2, \\ f_2(u), & u \in S_2 \subset \mathbb{R}^2, \end{cases}$$

where S_1 and S_2 are open sets, separated by a differentiable curve Σ, and the functions $f_1(u)$ and $f_2(u)$ are continuous.

In addition to *generic bifurcations* in continuous dynamical systems [6], Filippov's systems could present *sliding* bifurcations, where variations in the bifurcation parameter cause alterations in Σ. All possible bifurcations in two-dimensional Filippov systems were listed by Kuznetsov [7].

Filippov systems can be used to model the dynamics of harvested populations when they are below a critical threshold, as in the case of timber production in harvested forests or fishing activities, in order to create strategies that maximize their production without risking over-harvesting.

In this case, and assuming that the population does not interact with the environment, aging is density independent and recruitment is increasing but saturating with density, there is a simple model, proposed in [1], that describes the dynamics and is given by:

$$\begin{cases} \dot{x} &= & -(a+d_1)x + \dfrac{by}{c+y}, \\ \dot{y} &= & ax - [d_2 + f(y)]y, \end{cases} \tag{1}$$

with

$$f(y) = \begin{cases} qE, & \text{if} \quad y > P, \\ 0, & \text{if} \quad y < P, \end{cases}$$

where $y(t) \geq 0$ describes the adult individuals suitable for harvesting and reproduction, $x(t) \geq 0$ represents the young individuals, $a > 0$ is the aging rate of x, $b > 0$ is the maximun birth rate for each adult in a unit of time, $c > 0$ is the average rate of births regardless of environment, $q > 0$ is the catchability coefficient, $E > 0$ is harvesting effort and $d_1, d_2 > 0$ are the mortality rate of x and y, respectively.

The goal of this work is to study computational results for the cases of bifurcations indicated in a discontinuous model (1), shown in [1], when adults of the same species are not captured if they fall below a certain fixed population.

To provide the necessary background, in section 2, we follow [5, 4] and give a description of basic notions such as equilibria, tangency point, trajectories and periodic orbits in Filippov plane systems. In section 3 the model to be studied is presented under certain assumptions. In section 4, a global qualitative analysis is carried out for each vector field that makes up the proposed model. Based on this, section 5 provides a local and global analysis of the Filippov system. Finally, in section 6, a bifurcation analysis is performed on the model (1) with respect to two parameters: harvesting and protection of the population to interact.

2. Basic notions of Filippov systems

Let X and Y be vector fields of class C^r, with $r > 1$, in an open set $U \subset \mathbb{R}^2$ such that $(0,0) \in U$. Let $f : U \to \mathbb{R}$ be a function of class C^r, $r > 1$, such that $\operatorname{grad} f(x,y) \neq 0$ for all $(x,y) \in U$ and $\Sigma = f^{-1}(0) \cap U = \{(x,y) \in U : f(x,y) = 0\}$ an open and differentiable dividing curve which divides U into two open regions

$$\Sigma^+ = \{(x,y) \in U : f(x,y) > 0\} \quad \text{and} \quad \Sigma^- = \{(x,y) \in U : f(x,y) < 0\},$$

with $\overline{\Sigma^+}$ and $\overline{\Sigma^-}$ their closures.

According to [5], a Filippov planar system $Z = (X,Y)$ is a vector field defined by

$$Z(x,y) = \begin{cases} X(x,y), & (x,y) \in \Sigma^+ \\ Y(x,y), & (x,y) \in \Sigma^-, \end{cases}$$

where X and Y are of class C^r, $r > 1$, in $\overline{\Sigma^+}$ and $\overline{\Sigma^-}$, respectively.

In order to establish the dynamics given by the Filippov planar system $Z = (X,Y)$ on U, we need to denote the local trajectory $\varphi_Z(t,p)$ for a initial point $p \in U$. For this purpose, it is important to determine whether point p belongs to Σ^+, Σ or Σ^-.

If $p \in \Sigma^+$ or $p \in \Sigma^-$, the local trajectory in $Z = (X,Y)$, with initial point in p, is defined by a trajectory in the vector fields X or Y, respectively. However, a trajectory must also be defined for the initial points $p \in \Sigma$. To do this, considering $Xf(p) = \langle X(p), \operatorname{grad} f(p)\rangle$ and $Yf(p) = \langle Y(p), \operatorname{grad} f(p)\rangle$, Σ is divided into three disjoint regions given by:

- Crossing region: $\Sigma^c = \{p \in \Sigma : Xf(p) \cdot Yf(p) > 0\}$ as seen in Figure 1,
- Sliding region: $\Sigma^s = \{p \in \Sigma : Xf(p) < 0, Yf(p) > 0\}$ represented by Figure 2(a),
- Escaping region: $\Sigma^e = \{p \in \Sigma : Xf(p) > 0, Yf(p) < 0\}$ represented by Figure 2(b),

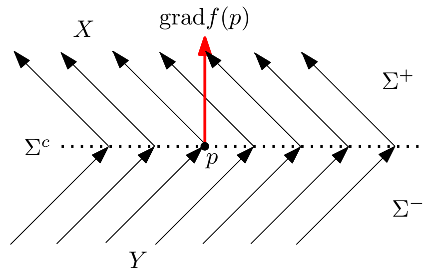

(a) $Xf(p)$, $Yf(p) > 0$. (b) $Xf(p)$, $Yf(p) < 0$.

FIGURE 1. Crossing region Σ^c.

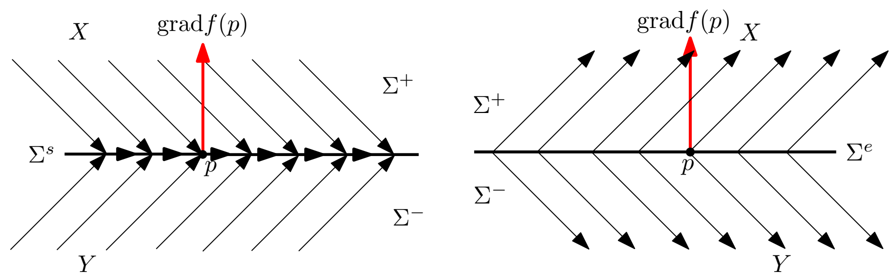

(a) Sliding region. (b) Escaping region.

FIGURE 2. Regions Σ^s and Σ^e.

If the boundary of the regions Σ^c, Σ^s or Σ^e are denoted by $\partial\Sigma^c$, $\partial\Sigma^s$ and $\partial\Sigma^e$, respectively, a point $p \in \partial\Sigma^c \cup \partial\Sigma^s \cup \partial\Sigma^e$, that is, $p \in \Sigma$ such that $Xf(p) = 0$ or $Yf(p) = 0$, is called a *tangency point*, and it can be classified as:

- *quadratic* if $Xf(p) = 0$ and $X^2f(p) = \langle X(p), \text{grad}Xf(p)\rangle \neq 0$, or $Yf(p) = 0$ and $Y^2f(p) = \langle Y(p), \text{grad}Yf(p)\rangle \neq 0$. A quadratic tangency $p \in \Sigma$ is *regular* if $Xf(p) = 0$, $X^2f(p) \neq 0$ and $Yf(p) \neq 0$; or $Yf(p) = 0$, $Y^2f(p) \neq 0$ and $Xf(p) \neq 0$. For the first case, a regular quadratic tangency is *visible* if $X^2f(p) > 0$ and *invisible* if $X^2f(p) < 0$ as seen in Figure 3(a). For the second case, $p \in \Sigma$ is visible if $Y^2f(p) < 0$ and invisible if $Y^2f(p) > 0$ as seen in Figure 3(b).
- *cubic* if $Xf(p) = X^2f(p) = 0$ and $X^3f(p) = \left\langle X(p), \text{grad}X^2f(p)\right\rangle \neq 0$ or $Yf(p) = Y^2f(p) = 0$ and $Y^3f(p) = \left\langle Y(p), \text{grad}Y^2f(p)\right\rangle \neq 0$, as seen in Figure 3(c).

We will now define the trajectory for an initial point p in Σ^c, Σ^s or Σ^e. As observed in Figure 1, in Σ^c, since both vector fields point either towards Σ^+ or Σ^-, it is enough to match the trajectories of X and Y through that point.

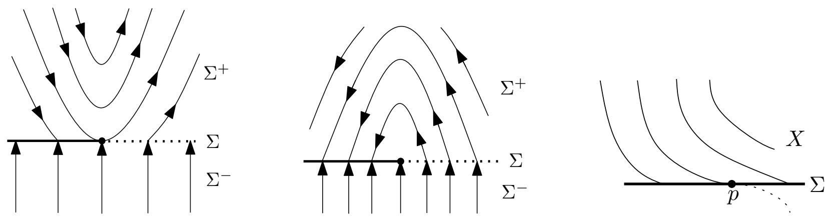

(a) Regular visible quadratic

(b) Regular invisible quadratic

(c) Cubic

FIGURE 3. Example of tangency points in $Z = (X, Y)$.

According to Filippov's method [7, 5], the trajectory in Σ^s or Σ^e is given by a convex combination of the vector fields X and Y tangent to Σ, that is,

$$Z^s(p) = \lambda(p)X(p) + (1 - \lambda(p))Y(p).$$

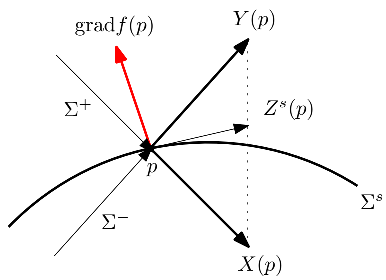

FIGURE 4. Construction of trajectories $Z^s(p)$.

In view of the Figure 4,

$$\langle Z^s(p), \mathrm{grad} f(p)\rangle = 0,$$

then

$$\lambda(p) = \frac{Yf(p)}{Yf(p) - Xf(p)}.$$

Therefore, the *sliding vector field* Z^s is given by

$$Z^s(p) = \frac{1}{Yf(p) - Xf(p)}(Yf(p)X(p) - Xf(p)Y(p)), \tag{2}$$

defined in $\Sigma^e \cup \Sigma^s$. For $p \in \Sigma^e \cup \Sigma^s$, the local trajectory of p is given by this vector field.

In $Z = (X, Y)$ the point $p \in \Sigma^s \cup \Sigma^e$ is called *pseudo-equilibrium* if $Z^s(p) = 0$, which is further classified as: *stable pseudo-node* if $p \in \Sigma^s$ and $(Z^s)'(p) < 0$

as shown in Figure 5(a), *unstable pseudo-node* if $p \in \Sigma^e$ and $(Z^s)'(p) > 0$ as shown in Figure Figure 5(b) and, *pseudo-saddle* if $p \in \Sigma^s$ and $(Z^s)'(p) > 0$, as seen in Figure 5(c), or $p \in \Sigma^e$ and $(Z^s)'(p) < 0$.

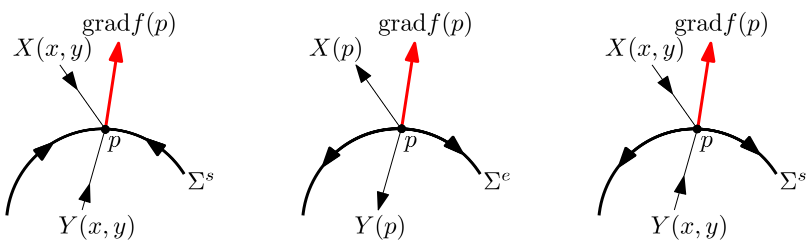

(a) stable pseudo-node (b) unstable pseudo-node (c) pseudo-saddle

FIGURE 5. Examples of pseudo-equilibrium in $Z = (X, Y)$

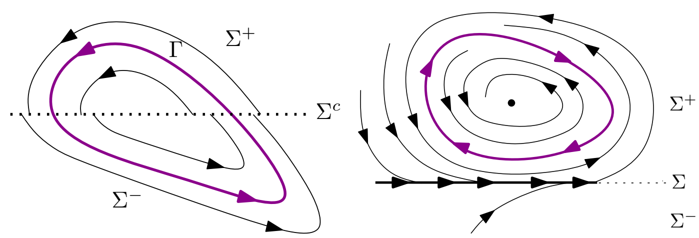

(a) Periodic orbit (b) Limit cycle

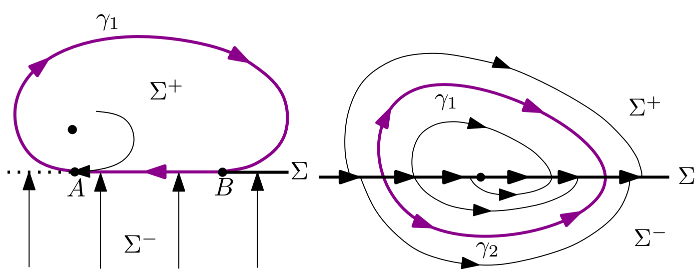

(c) Cycle (d) Pseudo-cycle

FIGURE 6. Examples of a periodic orbit, limit cycle, cycle, and a pseudo-cycle in $Z = (X, Y)$ represented by the purple curve. The black curves are trajectories that are not periodic.

Keeping in mind this background, the trajectory over the vector field of $Z = (X, Y)$ is defined as follows.

Definition 2.1. Let φ_X and φ_Y the trajectories in the vector fields X and Y defined for for $t \subset I \in \mathbb{R}$, respectively. The local trajectory φ_Z in $Z = (X, Y)$ through a point p is defined as follows:

- For $p \in \Sigma^+$ or $p \in \Sigma^-$ such that $X(p) \neq 0$ or $Y(p) \neq 0$ respectively, the trajectory is given by $\varphi_Z(t,p) = \varphi_X(t,p)$ or $\varphi_Z(t,p) = \varphi_X(t,p)$ respectively, for $t \subset I \in \mathbb{R}$.
- For $p \in \Sigma^c$ such that $Xf(p), Yf(p) > 0$, as shown in Figure 1(a), and taking the origin of time at p, the trajectory is defined as $\varphi_Z(t,p) = \varphi_Y(t,p)$ for $t \subset I \cap \{t \leq 0\}$ and $\varphi_Z(t,p) = \varphi_X(t,p)$ for $t \subset I \cap \{t \geq 0\}$. For the case $Xf(p), Yf(p) < 0$, as shown in Figure 1(a), the trajectory is defined as $\varphi_Z(t,p) = \varphi_Y(t,p)$ for $t \subset I \cap \{t \geq 0\}$ and $\varphi_Z(t,p) = \varphi_X(t,p)$ for $t \subset I \cap \{t \leq 0\}$.
- For $p \in \Sigma^e \cup \Sigma^s$ such that $Z^s(p) \neq 0$, the trajectory is given by $\varphi_Z(t,p) = \varphi_{Z^s}(t,p)$ for $t \in I \subset \mathbb{R}$, where Z^s is the sliding vector field given in (2).
- For $p \in \partial\Sigma^c \cup \partial\Sigma^s \cup \partial\Sigma^e$ such that the definitions of trajectories for points in Σ in both sides of p can be extended to p and coincide, the trajectory through p is this common trajectory. We will call these points *regular tangency points*.
- For any other point $\varphi_Z(t,p) = \{p\}$ for all $t \in I \subset \mathbb{R}$. This is the case of the tangency points in Σ which are not regular and which will be called *singular tangency points* and are the critical points of X in Σ^+, Y in Σ^- and Z^s in $\Sigma^e \cup \Sigma^s$.
- As observed in Figure 6(a), a *regular periodic orbit* is a orbit $\Gamma = \{\varphi_Z(t,p) : t \in \mathbb{R}\}$, which therefore belongs to $\Sigma^+ \cup \Sigma^- \cup \overline{\Sigma^c}$ such that $\varphi_Z(t+T,p) = \varphi_Z(t,p)$ for some $T > 0$.
- A *limit cycle* in Σ^+, or in Σ^-, is a limit cycle in $Z = (X, Y)$ which is represented in Figure 6(b).
- A *cycle* in $Z = (X, Y)$ is a limit cycle formed by the union of a sequence of curves $\gamma_1, \cdots, \gamma_n$, such that $\gamma_{2k} \subset \Sigma^s$ and $\gamma_{2k+1} \subset \Sigma^+ \cup \Sigma^-$, where the arrival and departure points belong to the closures of γ_{2k} and γ_{2k+1}, respectively. Figure 6(c) is an example of a cycle where $n = 2$.
- A *pseudo-cycle* is the union of a set of trajectories $\gamma_1, \cdots, \gamma_n$, contained in Σ^+ or Σ^-, such that the end point of some γ_i coincides with the end point of the next curve and the initial point of γ_i coincides with the initial point of the previous curve. Figure 6(d) shows a pseudo-cycle.

With the basic notions for Filippov systems, we can perform the qualitative analysis for the model (1).

3. Model Description

Assume that $w(t) \geq 0$ is the density of a species at time $t \geq 0$ and that it does not interact with any other species to subsist in an environment. Suppose that the population is divided into two groups: young individuals $x(t) \geq 0$ and adults individuals $y(t) \geq 0$, where only adults can reproduce and be caught only when found above a critical value P, that is, when $y > P$.

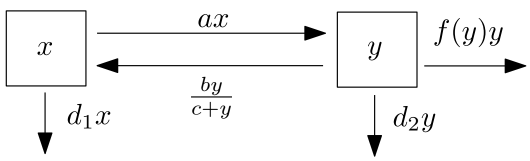

FIGURE 7. Model construction (5).

As observed in Figure 7 and if aging is density independent and recruitment is increasing but saturating with density, the evolution of young individuals x can be described by

$$\dot{x} = -(a + d_1)x + \frac{by}{c + y} \tag{3}$$

where $a > 0$ is the aging rate of x, $d_1 > 0$ is the mortality rate, $b > 0$ is the maximum birth rate for each adult by a unit of time and $c > 0$ is an auxiliary parameter affecting the general shape of the per capita growth curve of x. Similarly, the change in the amount of adult species y with respect to time $t \geq 0$ is given by

$$\dot{y} = ax - [d_2 + f(y)]y, \tag{4}$$

where $d_2 > 0$ is the mortality rate of the adult species y and

$$f(y) = \begin{cases} qE, & \text{if} \quad y > P, \\ 0, & \text{if} \quad y < P, \end{cases}$$

with $q > 0$ the catchability coefficient and $E > 0$ is harvesting effort.

Therefore, as in [1], this model is described by a Filippov system:

$$Z(x,y) = \begin{cases} X(x,y) = \begin{pmatrix} -(a+d_1)x + \dfrac{by}{c+y} \\ ax - (d_2 + qE)y \end{pmatrix}, & y > P \\ \\ Y(x,y) = \begin{pmatrix} -(a+d_1)x + \dfrac{by}{c+y} \\ ax - d_2 y \end{pmatrix}, & y < P \end{cases} \tag{5}$$

where

$$\begin{aligned} \Sigma^+ &= \{(x,y) \in \mathbb{R}^2 : x > 0, f(x,y) = y - P > 0\}, \\ \Sigma &= \{(x,y) \in \mathbb{R}^2 : x > 0, f(x,y) = y - P = 0\}, \\ \Sigma^- &= \{(x,y) \in \mathbb{R}^2 : x > 0, f(x,y) = y - P < 0\}. \end{aligned}$$

4. Qualitative analysis of the vector fields X and Y

First, note that the trajectories in vector fields X or Y remain in the region $\Omega = \left\{(x,y) \in \mathbb{R}^2 : x, y \geq 0\right\}$ as noted in the following result:

Lemma 4.1. *Ω is invariant under the vector field X or Y.*

Proof. For the case of the vector field X, if $x = 0$, $\dot{x} = \frac{by}{c+y} \geq 0$ for all $y \geq 0$. Similarly, if $y = 0$, $\dot{y} = ax \geq 0$ for all $x \geq 0$. This shows that the paths over the X field cannot cross the border of Ω and therefore Ω is invariant. A similar argument demonstrates the invariance of Ω under the vector field Y. ☑

On the other hand, the following result guarantees that the vector fields X and Y do not have limit cycles in Ω.

Lemma 4.2. *The vector fields X and Y do not have limit cycles in Ω.*

Proof. The vector field Y does not have limit cycles in Ω. Indeed, if

$$f(x,y) = -(a+d_1)x + b\frac{y}{c+y},$$

and

$$g(x,y) = ax - (d_2 + qE)y,$$

then

$$\frac{\partial f}{\partial x} + \frac{\partial g}{\partial y} = -(a + d_1 + d_2 + qE) < 0$$

for all $(x,y) \in \Omega$. By Bendixson-Dulac criterion [9], the vector field Y does not have limit cycles in Ω. A similar argument demonstrates that X does not have limit cycles in Ω. ☑

The equilibrium points of the vector field X are given by

$$Q_0^X = (0,0),$$

$$Q_*^X = \left(\frac{a[b - c(d_2+qE)] - cd_1(d_2+qE)}{a(a+d_1)}, \frac{a[b - c(d_2+qE)] - cd_1(d_2+qE)}{(d_2+qE)(a+d_1)}\right),$$

and the equilibrium of the vector field Y are

$$Q_0^Y = (0,0),$$

$$Q_*^Y = \left(\frac{a(b - cd_2) - cd_1d_2}{a(a+d_1)}, \frac{a(b - cd_2) - cd_1d_2}{d_2(a+d_1)}\right).$$

If $ab > c(d_2+qE)(a+d_1)$, and since $c(d_2+qE)(a+d_1) > cd_2(a+d_1)$, then $Q_*^X, Q_*^Y \in \Omega$. If $ab < cd_2(a+d_1)$, then $Q_*^X, Q_*^Y \notin \Omega$.

The Jacobian matrix of the vector field X evaluated at Q_0^X is given by

$$DX(Q_0^X) = \begin{bmatrix} -(a+d_1) & \dfrac{b}{c} \\ a & -(d_2+qE) \end{bmatrix},$$

with

$$\det DX(Q_0^X) \quad = \quad (a+d_1)(d_2+qE) - \frac{ab}{c},$$

and

$$\operatorname{tr} DY(Q_0^X) \quad = \quad -(a+d_1+d_2+qE) < 0.$$

If $ab > c(d_2+qE)(a+d_1)$ then Q_0^X is locally unstable. If $ab < c(d_2+qE)(a+d_1)$ then Q_0^X is locally stable.

The Jacobian matrix of the vector field Y evaluated at Q_0^Y is given by

$$DY(Q_0^Y) = \begin{bmatrix} -(a+d_1) & \dfrac{b}{c} \\ a & -d_2 \end{bmatrix},$$

with

$$\det DY(Q_0^Y) \quad = \quad (a+d_1)d_2 - \frac{ab}{c},$$

and

$$\operatorname{tr} DY(Q_0^Y) \quad = \quad -(a+d_1+d_2) < 0.$$

If $ab > cd_2(a+d_1)$ then $\det DY(Q_0^Y) < 0$ and, by Grobman-Hartman Theorem [9], Q_0^Y is locally unstable. However, if $ab < cd_2(a+d_1)$ then Q_0^Y is locally stable.

On the other hand, if $ab > cd_2(a+d_1)$, the Jacobian matrix in the vector field Y evaluated at Q_*^Y,

$$DY(Q_*^Y) = \begin{bmatrix} -(a+d_1) & \dfrac{cd_2^2(a+d_1)^2}{a^2b} \\ a & -d_2 \end{bmatrix},$$

with

$$\begin{aligned} \det DY(Q_*^Y) \quad &= \quad \frac{d_2(a+d_1)[a(b-cd_2)-cd_1d_2]}{ab} > 0, \\ \operatorname{tr} DY(Q_*^Y) \quad &= \quad -(a+d_1+d_2) < 0, \end{aligned}$$

and

$$\triangle = [\operatorname{tr} DY(Q_*^Y)]^2 - 4\det DY(Q_*^Y) > 0$$

because

$$\begin{aligned} ab(a+d_1+d_2)^2 \quad &> \quad d_2(a+d_1)(ab-acd_2-cd_1d_2) \\ &> \quad d_2(a+d_1)[cd_2(a+d_1)-acd_2-cd_1d_2] = 0. \end{aligned}$$

Thus, Q_*^Y is a locally stable node. Furthermore, since Ω is invariant and does not have limit cycles on the vector field Y, by the Poincaré - Bendixson Theorem [9], every trajectory in Y converges to the equilibrium Q_*^Y, and so Q_*^Y is a globally asymptotically stable equilibrium. Similarly, when substituting d_2 for $d_2 + qE$, then Q_*^X is a globally asymptotically stable equilibrium in the vector field X. Therefore, the following result has been proved.

Theorem 4.3. *If $ab < cd_2(a + d_1)$ then $Q_*^X, Q_*^Y \notin \Omega$ and Q_0^X or Q_0^Y are globally asymptotically stable equilibria on the vector field X or Y, respectively. If $ab > c(d_2 + qE)(a + d_1)$ then Q_*^X or Q_*^Y are globally asymptotically stable equilibria on the vector field X or Y, respectively.*

5. Qualitative analysis of the Filippov system $Z = (X, Y)$

For a qualitative analysis of the Filippov system (5), we will determine regions Σ^s, Σ^c, Σ^e and calculate the sliding vector field Z^s (2). Indeed, for all $p \in \Sigma$,

$$Xf(p) \quad = \quad \langle X(p), \mathrm{grad} f(p)\rangle \quad = \quad ax - (d_2 + qE)P,$$

and

$$Yf(p) \quad = \quad \langle Y(p), \mathrm{grad} f(p)\rangle \quad = \quad ax - d_2 P,$$

such that

$$Xf(p) \cdot Yf(p) = (ax - d_2P)(ax - (d_2 + qE)P) < 0,$$

and one of the following conditions must hold:

- $ax - d_2P > 0$ and $ax - (d_2 + qE)P < 0$, that is, $\frac{d_2 P}{a} < x < \frac{d_2+qE}{a}P$,
- $ax - d_2P < 0$ and $ax-(d_2+qE)P > 0$, equivalent to, $\frac{d_2+qE}{a}P < x < \frac{d_2}{a}P$.

However, the last condition does not occur since $\frac{d_2}{a} < \frac{d_2+qE}{a}$. Therefore,

$$\begin{aligned}
\Sigma^s &= \left\{(x, y) \in \mathbb{R}^2 : \frac{d_2 P}{a} < x < \frac{(d_2 + qE)P}{a}, y = P\right\},\\
\Sigma^c &= \left\{(x, y) \in \mathbb{R}^2 : x < \frac{d_2 P}{a} \text{ or } \frac{(d_2 + qE)P}{a} < x, y = P\right\},\\
\Sigma^e &= \varnothing.
\end{aligned}$$

The sliding vector field Z^s is given by

$$Z^s(p) = \begin{pmatrix} \dfrac{bP - x(a + d_1)(c + P)}{c + P} \\ \\ 0 \end{pmatrix},$$

with equilibria

$$PN = \left(\frac{bP}{(a+d_1)(c+P)}, P\right), \tag{6}$$

which corresponds to a stable pseudo-node, because for all $p \in \Sigma^s$,

$$\frac{\mathrm{d}}{\mathrm{d}x}\left(\frac{bP - x(a+d_1)(c+P)}{c+P}\right) = -(a+d_1) < 0.$$

The sliding segment has two tangency points, $Xf(p) = 0$ or $Yf(p) = 0$ with $p \in \Sigma$, given by

$$T_1 = \left(\frac{d_2}{a}P, P\right), \tag{7}$$

and

$$T_2 = \left(\frac{d_2 + qE}{a}P, P\right). \tag{8}$$

The tangency point T_2 is visible if

$$X^2 f(T_2) = \frac{P\{a[b - (c+P)(d_2+qE)] - d_1(c+P)(d_2+qE)\}}{c+P} > 0,$$

that is,

$$P < \frac{ab}{(a+d_1)(d_2+qE)} - c, \tag{9}$$

and invisible if $X^2 f(T_2) < 0$, that is,

$$P > \frac{ab}{(a+d_1)(d_2+qE)} - c. \tag{10}$$

Similarly, the tangency point T_1 is visible if

$$P > \frac{ab}{d_2(a+d_1)} - c \tag{11}$$

and invisible if

$$P < \frac{ab}{d_2(a+d_1)} - c. \tag{12}$$

As seen in Figure 8, PN is at the intersection of $\Sigma^s \equiv \overline{T_1T_2}$ and the nullclines $\dot{x}, \dot{y} = 0$.

If $ab > c(d_2 + qE)(a + d_1)$, that is $ab > cd_2(a + d_1)$, the equilibria Q_*^X, Q_*^Y and pseudo-equilibrium PN are not present simultaneously in the phase portrait of the Filippov system (5) as demonstrated by the following result:

Lemma 5.1. *If $ab > c(d_2 + qE)(a + d_1)$, the equilibria PN, Q_*^X and Q_*^Y do not coexist in the Filippov system* (5).

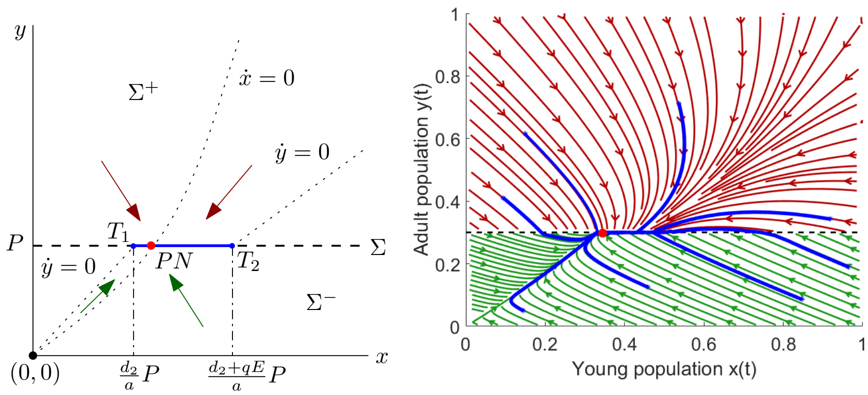

FIGURE 8. Nullclines $\dot{x} = 0$ and $\dot{y} = 0$, slidind segment $\overline{T_1T_2}$, PN and phase portrait of the Filippov system (5) with parameters: $a = c = d_1 = d_2 = q = E = 1$, $b = 3$, $P = 0.3$.

Proof. If the pseudo-node PN exists, that is $PN \in \overline{T_1T_2} \equiv \Sigma^s$, from (6), (7) and (8) we have that

$$\frac{d_2}{a} < \frac{b}{(a + d_1)(c + P)} < \frac{d_2 + qE}{a},$$

equivalenty,

$$\frac{ab}{(d_1 + a)(d_2 + qE)} - c < P < \frac{ab}{d_2(d_1 + a)} - c.$$

If $P < \frac{ab}{d_2(d_1+a)} - c$, then $\frac{a(b-cd_2)-cd_1d_2}{d_2(a+d_1)} > P$ and so $Q_*^Y \notin \Sigma^-$, that is, Q_*^Y is not defined for the Filippov system (5). Similarly, if $\frac{ab}{(d_1+a)(d_2+qE)} - c < P$, then $\frac{a[b-c(d_2+qE)]-cd_1(d_2+qE)}{(d_2+qE)(a+d_1)} < P$ and $Q_*^X \notin \Sigma^+$.

Conversely, if Q_*^Y belongs to the Filippov system (5), that is, $\frac{a(b-cd_2)-cd_1d_2}{d_2(a+d_1)} < P$, then $\frac{ab}{d_2(d_1+a)} - c < P$ and so $PN \notin \Sigma^s$. Similarly, if Q_*^X exist, then $\frac{ab}{(d_1+a)(d_2+qE)} - c > P$ and $PN \notin \Sigma^s$.

It remains to verify that Q_*^X and Q_*^Y do not coexist. Indeed, since

$$\frac{a(b - cd_2) - cd_1d_2}{d_2(a + d_1)} > \frac{a[b - c(d_2 + qE)] - cd_1(d_2 + qE)}{(d_2 + qE)(a + d_1)},$$

if Q_*^X exist, that is, $\frac{a[b-c(d_2+qE)]-cd_1(d_2+qE)}{(d_2+qE)(a+d_1)} > P$, then $P < \frac{a(b-cd_2)-cd_1d_2}{d_2(a+d_1)}$ and so $Q_*^Y \notin \Sigma^-$.

If Q_*^Y exists, that is, $\frac{a(b-cd_2)-cd_1d_2}{d_2(a+d_1)} < P$, then $\frac{a[b-c(d_2+qE)]-cd_1(d_2+qE)}{(d_2+qE)(a+d_1)} < P$ and so $Q_*^X \notin \Sigma^+$. ☑

We can now derive the following result using Theorem 4.3 and Lemma 5.1, as illustrated in Figures 8, 9, and 10.

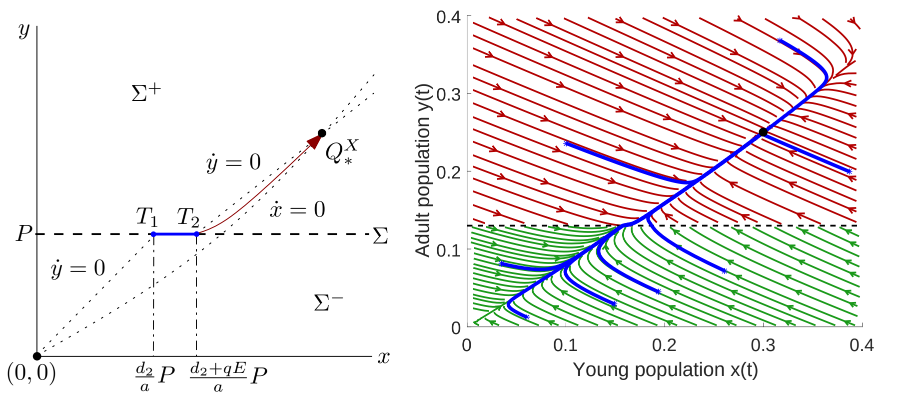

FIGURE 9. Nullclines $\dot{x}=0$ and $\dot{y}=0$, slidind segment $\overline{T_1T_2}$, Q_*^X and phase portrait of the Filippov system (5) with parameters: $a=c=d_1=d_2=q=1$, $E=0.2$, $b=3$, $P=0.13$.

Theorem 5.2. *If PN, Q_*^X or Q_*^Y exist in the Filippov system* (5)*, these are globally asymptotically stable nodes.*

However, if $ab < cd_2(a+d_1)$, that is Q_*^X and Q_*^Y does not exist in the Filippov system (5), the equilibrium Q_0^X and the pseudo-equilibrium PN are not defined in the Filippov system (5). Consequently, and as in Theorem 4.3, the equilibrium Q_0^Y is globally asymptotically stable in the Filippov system (5) for all $P, E > 0$ as observed in Figure 11.

Lemma 5.3. *If $ab < cd_2(a+d_1)$, then the equlibrium Q_0^X and the pseudo-equilibrium PN do not belong in the Filippov system* (5)*.*

Proof. Clearly, Q_0^X does not exist for system (5) since $P>0$. Similarly, if the pseudo-node PN exists, that is $PN \in \overline{T_1T_2} \equiv \Sigma^s$, then

$$\frac{d_2}{a} < \frac{b}{(a+d_1)(c+P)} < \frac{d_2+qE}{a},$$

equivalently,

$$\frac{ab}{(d_1+a)(d_2+qE)} - c < P < \frac{ab}{d_2(d_1+a)} - c.$$

Since $ab < cd_2(a+d_1)$, then $\frac{ab}{d_2(d_1+a)} - c < 0$ and therefore $P<0$, a contradiction. ☑

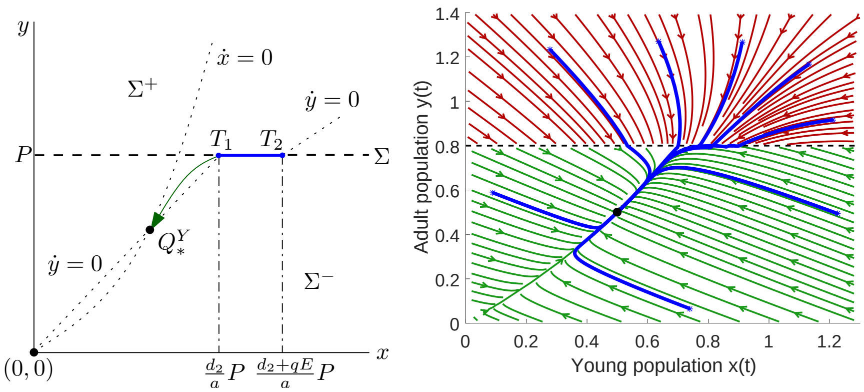

FIGURE 10. Nullclines $\dot{x}=0$ and $\dot{y}=0$, slidind segment $\overline{T_1T_2}$, Q_*^Y and phase portrait of the Filippov system (5) with parameters: $a=c=d_1=d_2=q=1$, $E=0.5$, $b=3$, $P=0.8$.

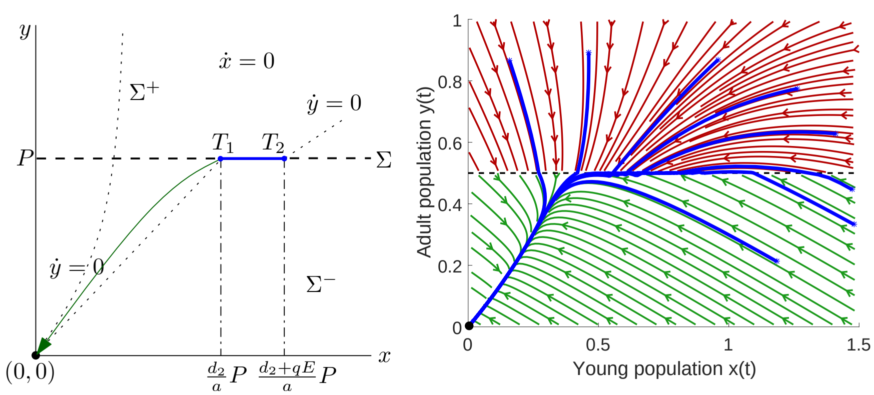

FIGURE 11. Nullclines $\dot{x}=0$ and $\dot{y}=0$, slidind segment $\overline{T_1T_2}$, Q_0^Y and phase portrait of the Filippov system (5) with parameters: $a=c=d_1=d_2=q=1$, $E=1$, $b=2$, $P=0.5$.

6. Bifurcation analysis

Finally, we analyze the cases in which the parameters E and P can significantly modify the phase diagrams for the Filippov system (5) through the collision of the elements found by the qualitative analysis given in section 5.

Clearly, for the case where $ab < cd_2(a+d_1)$, and in view of Lemma 5.3, the system (5) has a single globally asymptotically stable equilibrium Q_0^Y independently of the parameters P and E, as shown in Figure 11.

For the case that $ab > c(d_2+qE)(a+d_1)$, if PN exists in the Filippov system (5), a *collision of PN with* T_1 and a *collision of PN with* T_2 are characterized by $PN \equiv T_1$ and $PN \equiv T_2$, respectively, that is,

$$P = \frac{ab}{(d_1+a)d_2} - c, \tag{13}$$

and

$$P = \frac{ab}{(d_1+a)(d_2+qE)} - c, \tag{14}$$

which generates three bifurcation regions as seen in Figure 12(a). The bifurcation curves (13) and (14) intersect at the point $\left(0, \frac{ab}{(d_1+a)d_2} - c\right)$ and form a collision between T_1 and T_2, so PN and Σ^c are not defined in the Filippov system (5). Otherwise, the pseudo-node PN is formed through the intersection of the nullcline $\dot{x} = 0$ with the sliding vector field Z^s as seen in Figure 8. Likewise, if the nullcline $\dot{x} = 0$ intersects the nullcline $\dot{y} = 0$, the equilibrium Q_*^X or Q_*^Y is formed depending on whether the point of intersections is below or above Σ, respectively, as observed in Figures 9 and 10.

From (6), (7) and (8), the pseudo-node PN exists if $PN \in \overline{T_1T_2}$, that is,

$$\frac{ab}{(d_1+a)(d_2+qE)} - c < P < \frac{ab}{d_2(d_1+a)} - c.$$

In this case, the pseudo-node PN exists only in region 2, as shown in Figure 12(c).

From (9) and (10), the tangency point T_2 is visible in region 3, as shown in Figure 12(d), and invisible in regions 1 and 2, as shown in Figure 12(b,c) respectively. From (11) and (12), the tangency point T_2 is visible in region 1, as shown in Figure 12(b), and invisible in regions 2 and 3, as shown in Figure 12(c,d) respectively.

On the other hand, Q_*^Y is a point in the Filippov system (5) if $\frac{ab}{d_2(d_1+a)} - c < P$, and does not belong to the Filippov system (5) if $\frac{ab}{d_2(d_1+a)} - c > P$. From Figure 12, Q_*^Y exists in region 3 and does not exist in regions 1 and 2. Similarly, Q_*^X exists in region 1 since $\frac{ab}{(d_1+a)(d_2+qE)} - c < P$, and does not exist in regions 2 and 3.

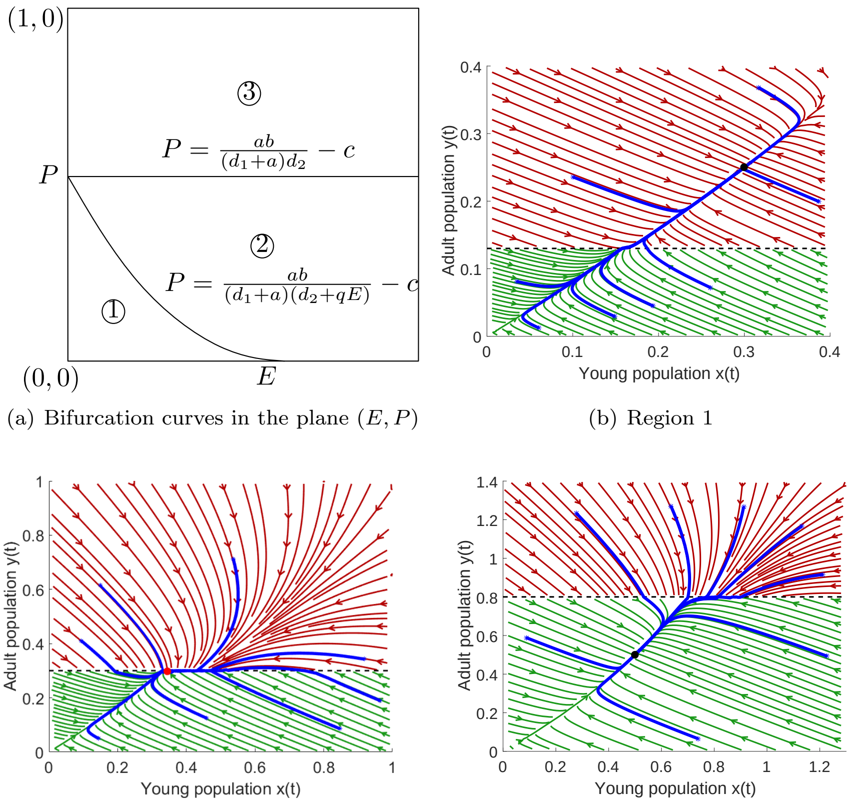

(a) Bifurcation curves in the plane (E, P)

(b) Region 1

(c) Region 2

(d) Region 3

Figure 12. Bifurcation diagram of the Filippov system (5) in the space (E, P), and phase portraits that characterize each region, for the following parameters: $a = c = d_1 = d_2 = q = 1$ and $b = 3$. Black point: $Q^*_{X,Y}$. Red point: PN.

To determine if there are more bifurcations in the Filippov system (5), it remains to verify the collision between T_1 and T_2. However, this is not possible since $\frac{d_2 P}{a} < \frac{(d_2+qE)P}{a}$. Therefore, Figure 12 shows the phase portraits for regions 1 to 4 of the Filippov system (5).

Conclusions

In this work, we analyze computational results for the different cases of bifurcations in the discontinuous model (5), proposed in [1]. The model (5) is used to analyze the dynamics of a species that is grown in a controlled environment, and isolated from predators, in order to harvest the adult species when it is above the threshold value, as in the case of timber production in harvested forests or fishing activities.

The existence of an internal equilibrium for model (5) is of vital importance in determining the overall stability of the system. If there is no internal equilibrium point in the X and Y fields, i.e., $ab < c(a + d_1)$, the species, young and adult, will go extinct over time, regardless of the threshold value P and the catching capacity of the adult species E. However, if $ab > c(a+d_1)$, the species will not go extinct, but will tend to stabilize over time, that is, it will tend in at least one equilibrium either of the X, Y or sliding field Z^s.

On the other hand, since the vector fields X and Y do not exhibit limit cycles, the complexity of showing the bifurcation cases for the Filippov system (5) is significantly reduced. This type of result means that the two groups of species do not exhibit a significant number of changes in their phase portrait. Since there are no periodic orbits, there will be no oscillations in the number of the two groups, hence the species should stabilize.

Since the bifurcation diagram shows all possible dynamics for the proposed model, if the objective is to control the species by increasing the level of catchability with low threshold of protection in the species so that it does not go extinct, in addition to the condition $ab > c(a + d_1)$, P and E should be chosen such that $\frac{ab}{(d_1+a)(d_2+qE)} - c < P < \frac{ab}{d_2(d_1+a)} - c$, that is, in region two.

Acknowledgments. This research was supported by MCIN/AEI/10.13039/501100011033 through grant BADS, no. PID2019-109320GB-100, and the associated FPI contract PRE2019-088899 to Christian Cortés García. The Spanish MICINN has also funded the "Severo Ochoa" Centers of Excellence to CNB, SEV 2017-0712.

References

[1] F. Dercole, A. Gragnani, and S. Rinaldi, *Bifurcation analysis of piecewise smooth ecological models*, Theoretical Population Biology **72** (2007), no. 2, 197–213.

[2] L. Edelstein-Keshet, *Mathematical models in biology*, SIAM, 2005.

[3] A. F. Filippov, *Differential equations with discontinuous righthand sides: control systems*, vol. 18, Springer Science & Business Media, 2013.

[4] C. Cortes Garcia, *Bifurcaciones en modelo gause depredador-presa con discontinuidad*, Revista de Matemática: Teoría y Aplicaciones **28** (2021), no. 2, 183–208.

[5] M. Guardia, T. M. Seara, and M. A. Teixeira, *Generic bifurcations of low codimension of planar Filippov systems*, Journal of Differential Equations **250** (2011), no. 4, 1967–2023.

[6] Y. A. Kuznetsov, *Elements of applied bifurcation theory*, vol. 112, Springer Science & Business Media, 2013.

[7] Y. A. Kuznetsov, S. Rinaldi, and A. Gragnani, *One-parameter bifurcations in planar Filippov systems*, International Journal of Bifurcation and chaos **13** (2003), no. 08, 2157–2188.

[8] J. D. Murray, *Mathematical biology: I. an introduction*, vol. 17, Springer Science & Business Media, 2007.

[9] J. Sotomayor, *Liçoes de equaçoes diferenciais ordinárias (vol. 11)*, Instituto de Matemática Pura e Aplicada, CNPq (1979).

(Recibido en abril de 2020. Aceptado en agosto de 2021)

Departamento de matemáticas
Universidad Carlos III de Madrid
Avenida de la Universidad, 30, 28911
Madrid, España
e-mail: chcortes@math.uc3m.es

Departamento de biología de sistemas
Centro Nacional de Biotecnología
Calle Darwin, 3, 28049
Madrid, España
e-mail: cc.cortes@cnb.csic.es

Departamento de matemática y estadística
Universidad Surcolombiana
Facultad de Ciencias Exactas y Naturales
Avenida Pastrana, calle 1
Neiva, Colombia
e-mail: juan.hernandez@usco.edu.co